MOLECULAR AND CELLULAR BIOLOGY, Feb. 2006, p. 1386–1397 Vol. 26, No. 4
0270-7306/06/$08.00+0 doi:10.1128/MCB.26.4.1386–1397.2006

Identification and Characterization of SAP25, a Novel Component of the mSin3 Corepressor Complex

Yuzuru Shiio,[1,2,3] David W. Rose,[4] Radin Aur,[4] Sam Donohoe,[2] Ruedi Aebersold,[2,5] and Robert N. Eisenman[1]*

Division of Basic Sciences, Fred Hutchinson Cancer Research Center, Seattle, Washington 98109-1024[1]; Institute for Systems Biology, Seattle, Washington 98103-8904[2]; Children's Cancer Research Institute, The University of Texas Health Science Center, San Antonio, Texas 78229-3900[3]; Department of Medicine and Cancer Center, University of California at San Diego, San Diego, California 92093-0673[4]; and Institute for Molecular Systems Biology, ETH-Zurich, and Faculty of Natural Sciences, University of Zurich, Zurich, Switzerland[5]

Received 5 July 2005/Returned for modification 25 July 2005/Accepted 25 November 2005

The transcriptional corepressor mSin3 is associated with histone deacetylases (HDACs) and is utilized by many DNA-binding transcriptional repressors. We have cloned and characterized a novel mSin3A-binding protein, SAP25. SAP25 binds to the PAH1 domain of mSin3A, associates with the mSin3A-HDAC complex in vivo, and represses transcription when tethered to DNA. SAP25 is required for mSin3A-mediated, but not N-CoR-mediated, repression. SAP25 is a nucleocytoplasmic shuttling protein, actively exported from the nucleus by a CRM1-dependent mechanism. A fraction of SAP25 is located in promyelocytic leukemia protein (PML) nuclear bodies, and PML induces a striking nuclear accumulation of SAP25. An isotope-coded affinity tag quantitative proteomic analysis of the SAP25 complex revealed that SAP25 is associated with several components of the mSin3 complex, nuclear export machinery, and regulators of transcription and cell cycle. These results suggest that SAP25 is a novel core component of the mSin3 corepressor complex whose subcellular location is regulated by PML.

mSin3A and mSin3B were originally identified as corepressors associated with the Mad family of transcriptional repressors (4, 48). Like their yeast ortholog Sin3p, mSin3 proteins have four imperfect repeats of a paired amphipathic helix (PAH) motif that mediate protein-protein interactions (56). Mad repression requires an interaction between the Sin3-interaction domain of Mad and the PAH2 domain of mSin3 (4, 6, 48). Sin3 corepressors are associated with histone deacetylases (HDACs), and the deacetylase activity is required for Sin3-mediated transcriptional repression (2, 18, 21, 23, 33, 42, 64).

mSin3A and mSin3B function as corepressors utilized by a growing number of transcriptional repressors such as MeCP2 (44), Ikaros (27), Pf1 (63), MNFβ (60), and Elk-1 (61). These mSin3-dependent transcriptional repressors function in diverse cellular processes, including proliferation, differentiation, apoptosis, and tumorigenesis. Recent genetic studies in mice have shown that mSin3A is an essential gene that is involved in cell fate determination (8, 9). Hence, understanding the function of the mSin3 complex will provide insight not only into the mechanism of mSin3/HDAC-dependent transcriptional repression but also into diverse aspects of cell behavior. In vivo, mSin3A is found associated with a large multiprotein complex containing HDAC1, HDAC2, RbAP46/48, SAP180, SAP130, SAP45/mSDS3, SAP30, SAP18, and other as yet uncharacterized proteins (1, 15, 18, 32, 64, 65). Some of these mSin3-binding proteins such as mSDS3 and SAP30 function as a "bridge" between the mSin3 complex and other protein complexes.

The broad elution pattern of the mSin3 complex from size exclusion columns (30, 52, 58) suggests that there are multiple mSin3 complexes containing different components in substoichiometric quantities. To fully understand the biological roles and regulation of mSin3 complexes, it is important to identify proteins that interact with mSin3. With this in mind, we have undertaken the identification of novel mSin3-binding proteins using λgt11 expression protein-protein interaction screening. Here we report the cloning and characterization of a novel mSin3A-binding protein, SAP25.

MATERIALS AND METHODS

cDNA cloning. A mouse 10-day-embryo cDNA library was purchased from Novagen. Lambda phage expression screens were carried out essentially as described previously (5, 24). His-tagged, full-length mSin3A protein was expressed using baculoviral infection of Sf9 cells. Glutathione *S*-transferase (GST)–PAH1, –PAH2, –PAH3, and –PAH4 were expressed in *Escherichia coli*. Purified proteins were ^{32}P labeled with heart muscle kinase (Sigma) and were used as probes for screening the plaque lifts.

Cell culture. 293, 293T, and BALB/c 3T3 cells were cultured in Dulbecco's modified Eagle's medium supplemented with 10% calf serum. HeLa cells, IMR-90 cells, and Rat1 cells were cultured in Dulbecco's modified Eagle's medium supplemented with 10% fetal calf serum. Calcium phosphate coprecipitation was used for transfection.

Northern blotting. Total cellular RNA was prepared as described previously (7). Twenty micrograms of total RNA was analyzed by Northern blotting. An adult mouse multiple-tissue Northern blot was purchased from Clontech.

Immunoprecipitation and immunoblotting. Immunoprecipitation and immunoblotting were performed as described previously (50). For metabolic labeling, the cells were incubated in methionine-free media for 30 min and labeled with 0.25 mCi/ml of [^{35}S]methionine for 4 h. Anti-SAP25 rabbit polyclonal antibody was raised against His-tagged, full-length SAP25 produced by baculoviral expression. A ca. 25-kDa protein band detected by immunoprecipitation of [^{35}S]Met-labeled cell lysates or by immunoblotting using this antibody can be blocked by preincubating the antibody with the immunogen, verifying the specificity of the antibody. Anti-HDAC2 was obtained from Ed Seto. Anti-mSin3A rabbit poly-

* Corresponding author. Mailing address: Division of Basic Sciences, Fred Hutchinson Cancer Research Center, 1100 Fairview Avenue North, Seattle, WA 98109-1024. Phone: (206) 667-4445. Fax: (206) 667-6522. E-mail: eisenman@fhcrc.org.

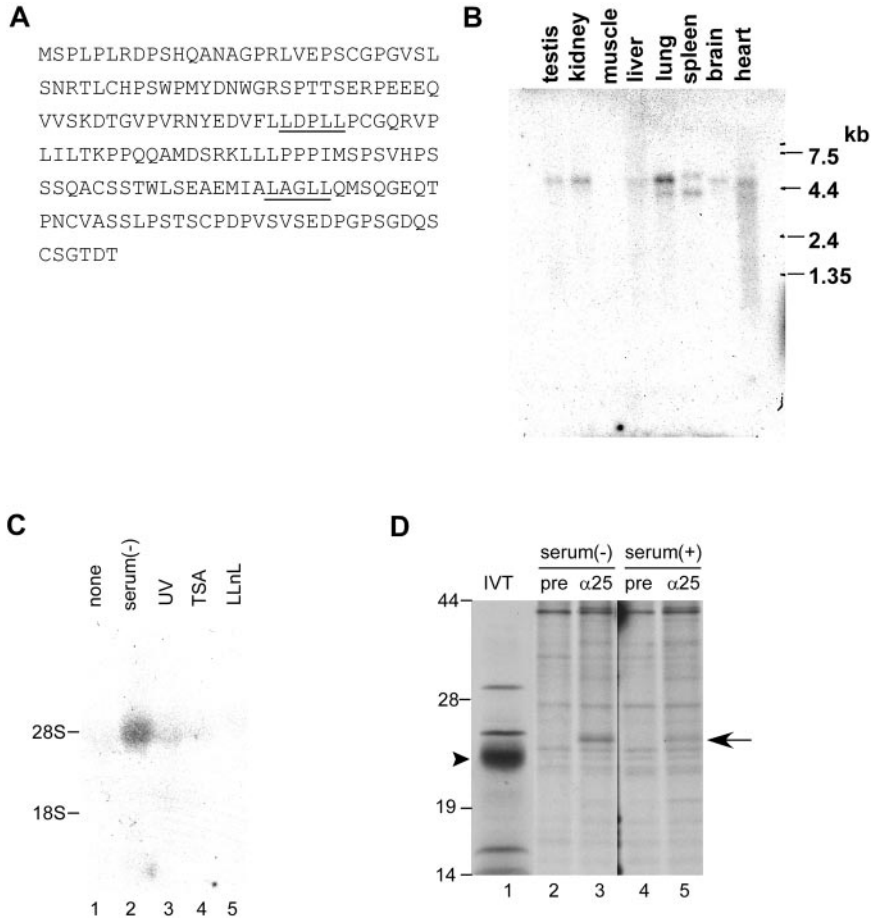

FIG. 1. Cloning of SAP25. (A) Deduced amino acid sequence of SAP25. The SAP25 open reading frame encodes a 186-amino-acid protein. The LXXLL motifs are underlined. (B) Tissue distribution of SAP25 mRNA expression. An adult mouse multiple-tissue Northern blot (Clontech) was probed with ^{32}P-labeled SAP25 cDNA fragment. (C) SAP25 mRNA expression upon different stimuli. Mouse BALB/c3T3 fibroblasts were deprived of serum overnight (lane 2) and treated with UV light (3.5 h after 254-nm UV irradiation at 1 mJ/cm^2) (lane 3), HDAC inhibitor TSA (1 ng/ml overnight) (lane 4), or proteasome-inhibitor LLnL (50 μM overnight) (lane 5), and SAP25 mRNA expression was examined by Northern blotting. (D) Induction of SAP25 protein expression upon serum starvation. Mouse BALB/c3T3 fibroblasts cultured with (lanes 4 and 5) or without (lanes 2 and 3) serum were labeled with [^{35}S]Met, and tricarboxylic acid-insoluble count-normalized lysates were immunoprecipitated with anti-SAP25 antibody (lanes 3 and 5) or with preimmune serum (lanes 2 and 4). The arrow indicates the position of endogenous SAP25 protein, which migrates slightly slower than the in vitro-translated (IVT) SAP25 (lane 1, arrowhead).

clonal antibody was raised against GST-PAH2. Anti-mitogen-activated protein kinase (anti-MAPK) antibody was obtained from Yoshiro Maru. Anti-Myc antibody was prepared from 9E10 hybridoma ascites fluid. Anti-FLAG M2 monoclonal antibody was purchased from Sigma.

ICAT proteomic analysis of SAP25 complex. HeLa cells (50 10-cm plates each) were transfected with FLAG-SAP25 alone or FLAG-SAP25 plus promyelocytic leukemia protein (PML). Forty-eight hours after transfection, the cell lysates were immunoprecipitated with anti-FLAG antibody under nondenaturing conditions and the precipitated proteins were eluted with FLAG peptide. The two protein complexes (ca. 70 μg each) were labeled with the cleavable isotope-coded affinity tag (ICAT) reagents (isotopically light ICAT for the FLAG-SAP25 sample and isotopically heavy ICAT for the FLAG-SAP25-plus-PML sample). The labeled protein mixtures were combined and proteolyzed to peptides with trypsin. The peptides were fractionated by cation-exchange chromatography (using an SCX cartridge from Applied Biosystems), followed by avidin affinity chromatography (using a monomeric avidin cartridge from Applied Biosystems). The isolated ICAT-labeled peptides were analyzed by microcapillary liquid chromatography-tandem mass spectrometry as described previously (16, 17, 49, 51). The amino acid sequences of the peptides were determined by correlating the collision-induced dissociation spectra with the protein sequence database using the SEQUEST search algorithm (13). The accuracy of peptide/protein identification was statistically validated by using the Peptide Prophet (25) and Protein Prophet (45) software tools. The relative abundance (FLAG-SAP25 alone versus FLAG-SAP25 plus PML) of an identified ICAT-labeled peptide pair was determined from the ratio of the peptide peaks using the ASAPRatio software tool (39).

Immunofluorescence. Immunofluorescence was performed as described previously (49). Anti-human PML 5E10 monoclonal antibody was obtained from Roel van Driel.

GST pulldown assay. In vitro-translated, [^{35}S]Met-labeled protein was incubated with 5 μg of purified GST fusion protein in 1× phosphate-buffered saline containing 0.4% NP-40 for 1 h at 4°C and washed three times, and bound proteins were analyzed by sodium dodecyl sulfate-polyacrylamide gel electrophoresis (SDS-PAGE).

Luciferase assay. The 4× GAL14D luciferase was described previously (3). The luciferase assay was performed as described in reference 50.

Microinjection reporter assay. The microinjection experiments (32) were performed in NIH 3T3 cells that had been serum deprived overnight prior to injection. For the antibody experiments, the DNA constructs were added at 100 μg/ml to either preimmune rabbit immunoglobulin G (IgG) or purified IgG raised against SAP25. Injected cells were detected by staining after incubation with tetramethyl rhodamine isothiocyanate (TRITC)-labeled donkey anti-rabbit IgG (Jackson Laboratories). Small interfering RNAs (siRNAs) were coinjected at a concentration of 50 nM with rhodamine-conjugated dextran (Molecular

Probes). The target sequence of SAP25 siRNA was 5′-CTTCCTGGCCGATGT ATGA-3′. Cells were fixed and stained overnight with X-Gal (5-bromo-4-chloro-3-indolyl-β-D-galactopyranoside) 24 h after injection for the antibody experiments and 48 h after injection for the siRNA experiments. LacZ expression was quantitated on an epifluorescence microscope. Each fluorescent-injected cell was individually scored as positive or negative for reporter expression, with any degree of staining for LacZ denoted as positive. Two hundred to 300 cells were injected for each experimental parameter, and each experiment was repeated at least three times. Results are expressed as percent blue cells, which represents the mean of all experiments + standard error.

RESULTS

Identification of SAP25. SAP25 cDNA was isolated in two λgt11 expression screens (5) with either baculovirus-produced full-length mSin3A or the mixture of bacterial GST-PAH1, -2, -3, and -4 as probes using a mouse 10-day-embryo cDNA library (Novagen). In each case, 2.4×10^6 plaques were screened and one clone, containing an open reading frame (ORF) encoding 186 amino acids, was isolated (Fig. 1A). This ORF is preceded by an in-frame stop codon, and the sequence surrounding the putative initiation codon conforms to the start codon consensus sequence (28). The SAP25 cDNA sequence is nearly identical to the 3′ portion of RIKEN cDNA 2810008P14 (IMAGE: 5353990). The deduced SAP25 amino acid sequence contains two LXXLL motifs. Such motifs have been previously implicated in the binding of steroid receptor coactivators with nuclear hormone receptors or cyclin D1 (20, 66). There is a human SAP25 homologue (FLJ00248 protein), and the C-terminal LXXLL motif and surrounding sequences are well conserved, although the N-terminal LXXLL motif is changed to SXXLL in human SAP25. Except for the LXXLL motifs, the SAP25 amino acid sequence does not contain any recognizable sequence motifs and does not display any significant homology to other proteins in the database.

Northern blot analysis demonstrated that SAP25 is widely expressed in adult mouse tissues (Fig. 1B). The predominant mRNA detected is between 4 and 5 kb, considerably larger than the putative SAP25 ORF. This raised the possibility that there might be alternatively spliced larger ORF(s) for SAP25. However, exhaustive screening (9×10^6 plaques) of a mouse lung cDNA library (Novagen) revealed only minor alternatively spliced isoforms that encode shorter ORFs, with no evidence of longer ORFs (data not shown). The presence of a long (3.5 to 4.5 kb) 5′ noncoding region suggests that SAP25 expression may be regulated at the level of translation (47).

SAP25 RNA and protein expression was found to be induced upon serum starvation of BALB/c3T3 fibroblasts (Fig. 1C and D), which may suggest a role of SAP25 in cell cycle arrest. UV, a histone deacetylase inhibitor, trichostatin A (TSA), and a proteasome inhibitor, LLnL, did not have any effect on SAP25 mRNA expression (Fig. 1C).

In vitro interaction of SAP25 and mSin3A. To map the SAP25-binding domain on mSin3A, we examined the binding of a series of C-terminal deletion mutants of mSin3A to GST-SAP25. As shown in Fig. 2A, all the C-terminal deletion mutants up to N205 bind to GST-SAP25. Note that although the full-length and N680 deletion mutant mSin3A displayed some binding to GST alone, they displayed clearly more binding to GST-SAP25. N205 contains the N-terminal sequence, including the PAH1 domain. The requirement of the PAH1 domain for SAP25 binding was examined by deleting the PAH1 domain from mSin3A. As shown in Fig. 2B, an mSin3A N-terminal deletion mutant that lacks the PAH1 domain does not bind, whereas full-length mSin3A and the N-terminal fragment containing the PAH1 domain bind GST-SAP25. The binding of the PAH1 domain to SAP25 was further confirmed by the interaction of full-length SAP25 and GST-PAH1 (Fig. 2C). The two bands detected for in vitro-translated SAP25 in Fig. 2C are likely due to internal initiation of translation.

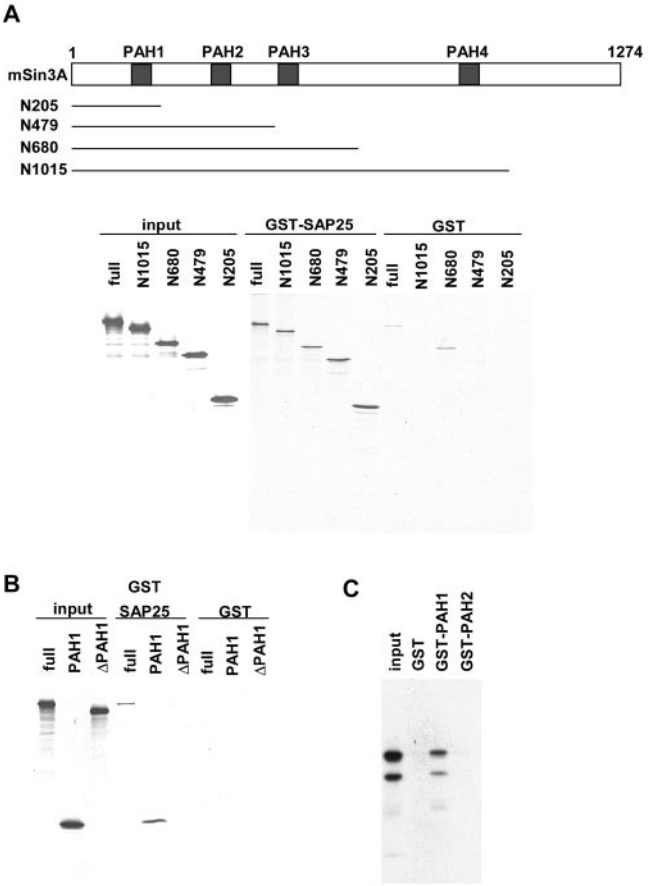

FIG. 2. Interaction of SAP25 and the PAH1 domain of mSin3A. (A) Interaction of C-terminal deletion mutants of mSin3A with GST-SAP25. The indicated mSin3A C-terminal deletion mutants were in vitro translated, [^{35}S]Met labeled, and incubated with GST-SAP25 or GST attached to glutathione agarose beads. The bound proteins were analyzed by SDS-PAGE. Input lanes contain 20% of the input to the binding reaction. (B) Requirement for the PAH1 domain of mSin3A for SAP25 binding. Full-length mSin3A (full), an mSin3A N-terminal 205-amino-acid fragment that contains the PAH1 domain (PAH1), or the mSin3A N-terminal deletion mutant that lacks the PAH1 domain (ΔPAH1, deletion of the N-terminal 206 amino acids) was analyzed for GST-SAP25 binding as in panel A. Input lanes contain 20% of the input to the binding reaction. (C) Interaction of SAP25 with the PAH1 domain. Full-length SAP25 protein was analyzed for binding to GST, GST-PAH1, or GST-PAH2 as in panel A. Input lanes contain one-seventh of the input to the binding reaction.

To map the mSin3A-binding domain on SAP25, we examined the binding of SAP25 deletion mutants to GST-PAH1. As shown in Fig. 3A, an N-terminal deletion mutant that retains the C-terminal one-third of SAP25 (residues 125 to 186) binds to GST-PAH1, whereas the deletion mutants that lack the C-terminal one-third of SAP25 (positions 1 to 62 and 1 to 124)

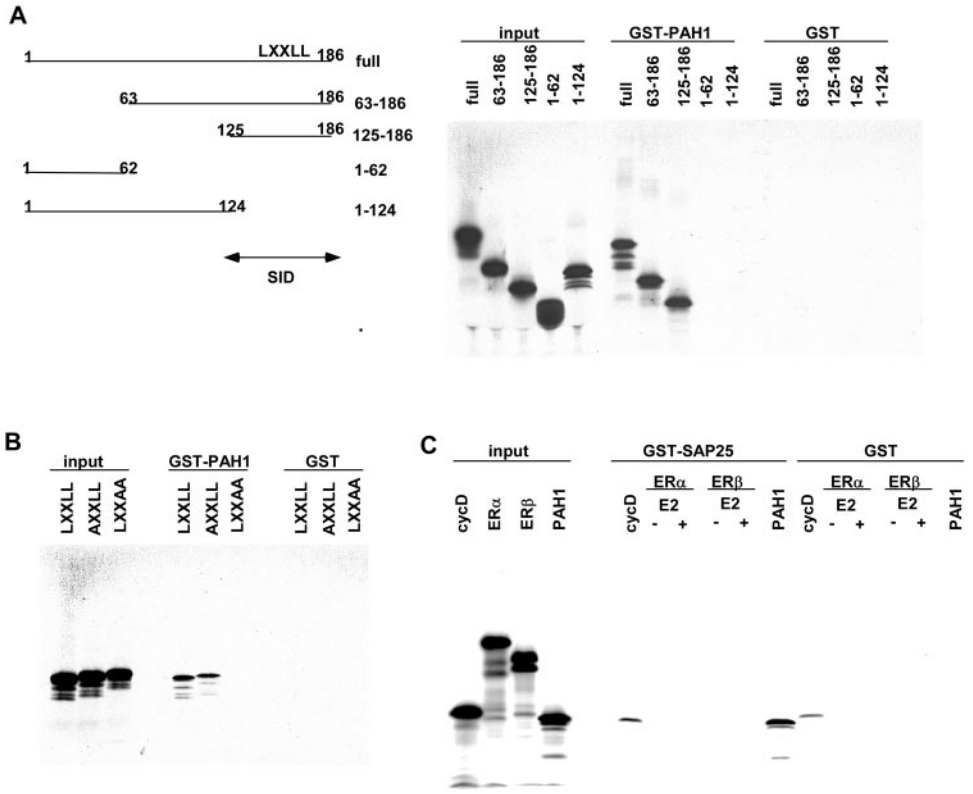

FIG. 3. Role of the LXXLL motif of SAP25 in binding to mSin3A PAH1. (A) Interaction of the deletion mutants of SAP25 with GST-PAH1. The indicated SAP25 deletion mutants were analyzed for binding to GST-PAH1 or GST as in Fig. 2A. The input lanes contain 20% of the input to the binding reaction. The *S*in3 *i*nteraction *d*omain (SID) of SAP25 is located in the C-terminal one-third of the protein (positions 125 to 186). (B) Requirement of the C-terminal LXXLL motif of SAP25 for binding to the PAH1 domain of mSin3A. Wild-type SAP25 or the SAP25 mutants that have mutations in the C-terminal LXXLL motif (LAGLL→AAGLL or LAGLL→LAGAA) were analyzed for binding to GST-PAH1. Input lanes contain 20% of the input to the binding reaction. (C) Specific interaction of SAP25 LXXLL motif with mSin3A PAH1. Cyclin D1, estrogen receptor α (ERα), estrogen receptor β (ERβ), or mSin3A PAH1 fragment was analyzed for binding to GST-SAP25 or GST alone. The interaction of ERα and ERβ was examined in both the presence and absence of the ligand (E2).

fail to bind. The slight difference in mobility between input and GST-bound proteins is likely due to the different buffer compositions of input and GST-bound samples. The different mobilities of the similarly sized 125-186 and 1-62 fragments probably reflect their different proline and charged amino acid (high in the 1-62 fragment) contents (see Fig. 1A). Our binding data indicate that the C-terminal one-third of SAP25 is necessary and sufficient for mSin3A binding. This region of SAP25 contains one of the LXXLL motifs (referred to here as the C-terminal LXXLL motif). To examine the importance of this LXXLL motif in the binding to PAH1, we introduced amino acid substitutions. As shown in Fig. 3B, the substitution of the first Leu of LXXLL to Ala (AXXLL) shows diminished binding and the replacement of the last two Leu to Ala (LXXAA) completely abolishes the binding to GST-PAH1, indicating that the C-terminal LXXLL motif is involved in the binding to PAH1. The slight difference in mobilities of the LXXLL mutants is reproducible; however, the reason for this difference is unknown. Consistent with the identification of the C-terminal LXXLL motif as an mSin3A binding domain, this LXXLL motif and the surrounding sequences are the only region of SAP25 that can assume α-helical structure (I. Radhakrishnan, personal communication).

LXXLL motifs of steroid receptor coactivators were shown to mediate their interactions with nuclear hormone receptors or cyclin D1 (20, 66). This prompted us to examine the interaction of SAP25 with nuclear hormone receptors or cyclin D1. As shown in Fig. 3C, SAP25 does not display significant interaction over the GST background with cyclin D1, estrogen receptor α, or estrogen receptor β, indicating that the LXXLL motif of SAP25 is relatively specific for binding to the PAH1 domain of mSin3A. Such interaction specificity for LXXLL motifs has been previously described (19, 66), although the determinants of specificity have not been clearly defined.

In vivo interaction of SAP25 and mSin3A complex. To determine if SAP25 binds to other cellular proteins in vivo, we transfected FLAG-tagged SAP25 into 293T cells, metabolically labeled the cells with [^{35}S]methionine, and performed immunoprecipitation under nondenaturing conditions. As shown in Fig. 4A, FLAG-SAP25 was expressed as a ca. 26-kDa protein and coimmunoprecipitated with several cellular proteins. A doublet of ca. 150 kDa and a band of ca. 60 kDa are approximately the expected sizes of endogenous mSin3A and HDAC, respectively (4, 18, 64). This was confirmed by analyzing the FLAG-SAP25 immunoprecipitate by immunoblotting. As shown

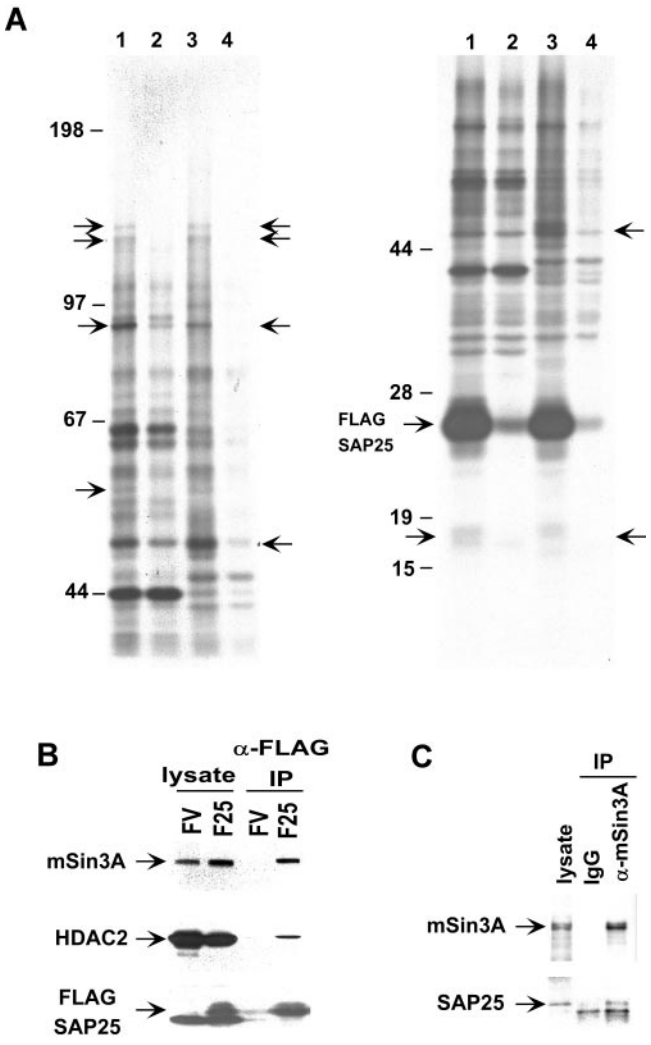

FIG. 4. Interaction of SAP25 with mSin3A complex in vivo. (A) Interaction of FLAG-SAP25 with cellular proteins. FLAG-SAP25 or FLAG empty vector was transfected into 293T cells. Two days later, the cells were labeled with [^{35}S]Met, lysed in TNE buffer (lanes 1 and 2) or high-salt buffer (lanes 3 and 4), immunoprecipitated with anti-FLAG antibody, and analyzed by 7.5% (left) or 15% (right) SDS-PAGE. Lanes 1 and 3 contain FLAG-SAP25 samples, and lanes 2 and 4 contain FLAG empty vector samples. FLAG-SAP25 was expressed as a ca. 26-kDa protein. The proteins coimmunoprecipitated with FLAG-SAP25 are marked with arrows. (B) Interaction of FLAG-SAP25 with mSin3A and HDAC2 in 293 cells. FLAG-SAP25 (F25) or FLAG empty vector (FV) was transfected into 293 cells. Two days later, the cells were lysed in TNE buffer and immunoprecipitated (IP) with anti-FLAG (α-FLAG) antibody. The cell lysates and immunoprecipitates were analyzed by anti-mSin3A, anti-HDAC2, or anti-FLAG immunoblotting. (C) Interaction of endogenous mSin3A and SAP25 in 293 cells. 293 cell lysates were immunoprecipitated with anti-mSin3A antibody or preimmune serum, and the immunoprecipitates were analyzed by anti-mSin3A (top) and anti-SAP25 (bottom) immunoblotting.

in Fig. 4B, endogenous mSin3A and HDAC2 coimmunoprecipitate with FLAG-SAP25 from 293 cells. Furthermore, association of endogenous mSin3A and endogenous SAP25 in 293 cells was confirmed by anti-mSin3A immunoprecipitation followed by anti-SAP25 immunoblotting (Fig. 4C).

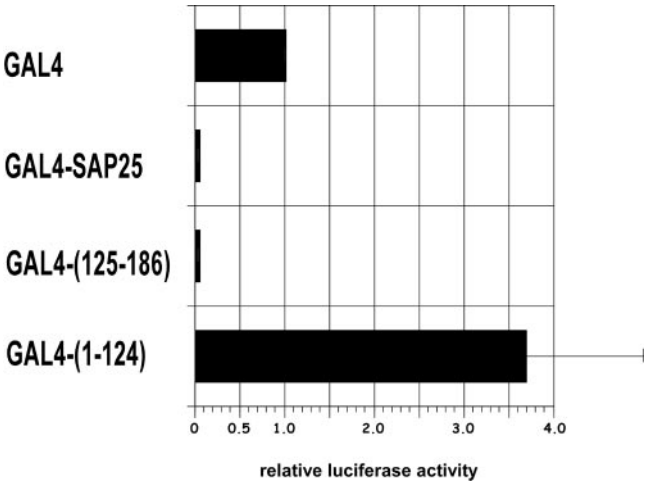

FIG. 5. Transcriptional repression by GAL4-SAP25. HeLa cells were cotransfected with 4× GAL14D-luciferase reporter and GAL4 vector, GAL4-SAP25, GAL4-SAP25(125-186), or GAL4-SAP25(1-124). The luciferase activities were determined 48 h after transfection. Transfection efficiency was normalized using a β-galactosidase assay. The data represent the average of three independent experiments.

If SAP25 associates with mSin3, it would be expected to possess repression activity when recruited to DNA. To test this, we fused a full-length SAP25 or deletion mutants of the SAP25 ORF to a GAL4 DNA-binding domain and examined their transcriptional activities. As shown in Fig. 5, GAL4-SAP25 or GAL4-SAP25 (125-186), which contains the mSin3A-binding domain, strongly represses transcription, whereas the deletion of the mSin3A-binding domain [GAL4-SAP25(1-124)] abolishes this repression. In fact GAL4-SAP25(1-124) activated transcription, which raises the possibility of an interaction between SAP25 and some transcriptional activation components (see below).

We also investigated the stability of SAP25 and found that SAP25 is a stable protein with a half-life of more than 4 h (data not shown). These results indicate that SAP25 is a stable protein that can interact with mSin3-HDAC complex and repress transcription in vivo.

Involvement of SAP25 in mSin3A-mediated repression. The functional significance of SAP25 association with mSin3A complex was examined by live cell microinjection reporter assays (Fig. 6) (32). GAL4-mSin3A represses transcription of 3XUAStk/lacZ reporter, as previously observed (32). Microinjection of anti-SAP25 antibody completely abolishes repression by GAL4-mSin3A, indicating that SAP25 is required for mSin3A-mediated repression. In contrast, microinjection of anti-SAP25 antibody does not affect repression by GAL4-N-CoR, which is consistent with the lack of interaction between SAP25 and N-CoR both in vitro and in vivo (Y. Shiio and R. N. Eisenman, unpublished data). Microinjection of anti-SAP25 antibody does not affect the basal and liganded activities of retinoic acid receptor, estrogen receptor, thyroid hormone receptor, and progesterone receptor (data not shown). This is consistent with the specific recruitment of N-CoR/SMRT, but not mSin3A, by thyroid hormone receptor (38). GAL4-SAP25 represses transcription of 3XUAStk/lacZ reporter, and this repression is abolished by microinjection of mSin3A antibody (Fig. 6), which is consistent with the requirement for the

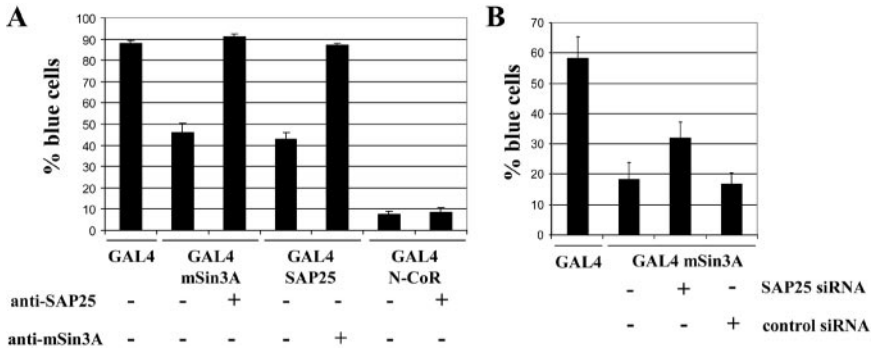

FIG. 6. SAP25 mediates repression by mSin3A (A) Repression of the 3XUAStk/lacZ reporter by the indicated GAL4-mSin3A, GAL4-N-CoR, or GAL4-SAP25 fusion proteins was assayed in microinjected NIH 3T3 cells. Anti-SAP25 or anti-mSin3A was coinjected as indicated. As a negative control, we used preimmune rabbit IgG, which did not affect the fraction of X-Gal-positive cells. Fold repression was determined by comparing the percentage of X-Gal-positive, injected cells in the presence of GAL4-mSin3A, GAL4-N-CoR, or GAL4-SAP25 relative to GAL4 alone. Two hundred to 300 cells were injected for each experimental parameter. The results are the average of two experiments performed in triplicate. (B) Repression of the 3XUAStk/lacZ reporter by GAL4-mSin3A was assayed in microinjected NIH 3T3 cells. SAP25 siRNA or control scrambled siRNA was coinjected as indicated.

mSin3A-binding domain in GAL4-SAP25-mediated repression (Fig. 5). To further confirm the role of SAP25 in mSin3A-mediated repression, we microinjected SAP25 siRNA or control siRNA and analyzed their effects on GAL4-mSin3A repression. As shown in Fig. 6B, SAP25 siRNA (see Materials and Methods), but not control siRNA, partly relieved GAL4-mSin3A repression. Taken together our results indicate that SAP25 is involved in mSin3A-mediated, but not N-CoR-mediated, repression.

Nuclear export of SAP25. When we examined the subcellular location of transfected FLAG-SAP25, we found that it is predominantly cytoplasmic (Fig. 7B). We noticed that the LXXLL motifs and the surrounding sequences of SAP25 are similar to the leucine-rich nuclear export signal (NES) (Fig. 7A). Although the degree of similarity to other known NESs is not high, very divergent leucine-rich sequences are known to function as NESs (29, 31). When we treated FLAG-SAP25-transfected cells with leptomycin B, an inhibitor of CRM1-dependent nuclear export, FLAG-SAP25 accumulated in nuclei (Fig. 7B). This indicates that SAP25 is actively exported from the nucleus by a CRM1-dependent mechanism. We next mapped the NES(s) in SAP25 by deletion and mutation analyses (Fig. 7C). The N-terminal deletion analysis of SAP25 indicated that the C-terminal one-third of the protein residues 125 to 186) is sufficient for nuclear export. Mutation of the C-terminal LXXLL motif [SAP25(125-186)-LXXAA] abolishes export. This indicates that there is an NES that overlaps with the C-terminal LXXLL motif. However, mutation of the C-terminal LXXLL motif or the deletion of the C-terminal one-third of SAP25 in the context of a full-length protein (SAP25-LXXAA and SAP25 residues 1 to 124) did not completely abolish the nuclear export. Because deletion of the C-terminal two-thirds of SAP25(1-62) abolishes nuclear export, there is likely to be a second NES in the central one-third of SAP25. Indeed, there is a second (N-terminal) LXXLL motif in this region (Fig. 1A), which may serve as a second NES for SAP25.

To investigate the possible consequences of SAP25 nuclear export, we examined the effect of SAP25 on the subcellular location of mSin3A. As shown in Fig. 7D, coexpression of SAP25 partially sequestered mSin3A in the cytoplasm. SAP25 may constantly shuttle between the nucleus and the cytoplasm, thereby regulating the nuclear pool of mSin3A.

The predominantly cytoplasmic localization of FLAG-SAP25 as determined by immunofluorescence prompted us to examine the subcellular location of SAP25 by biochemical fractionation. As shown in Fig. 7E, although the majority of FLAG-SAP25 was located in the cytoplasm, a significant fraction was present in the nucleus and cofractionates with Myc, which is exclusively nuclear and serves as a positive control. The nuclear fraction of SAP25, which can interact with nuclear mSin3A, is likely to be regulated by CRM1-dependent nuclear export. SAP25 may also have an mSin3A-independent role in the cytoplasm.

Localization of SAP25 to PML nuclear bodies. Immunofluorescent staining of endogenous SAP25 in HeLa cells revealed that it is mainly cytoplasmic, but a fraction of SAP25 is located in the nucleus and is concentrated in nuclear dot-like structures which coincide with the PML nuclear bodies (Fig. 8A, top row). Leptomycin B treatment caused accumulation of SAP25 in the PML nuclear bodies (Fig. 8A, second row). Although SAP25 mRNA and protein are induced by serum starvation (Fig. 1C and D), serum starvation does not affect the subcellular location of SAP25 (data not shown). Transfected SAP25 was predominantly cytoplasmic, but coexpression of PML caused accumulation of SAP25 in the PML nuclear bodies (which are enlarged by overexpression of PML) and the nucleoplasm (Fig. 8A, third and fourth rows). The PML nuclear bodies increase in size and number upon Ras-induced senescence of primary fibroblasts and play a pivotal role in this process (14, 46). Thus, we examined the subcellular location of SAP25 upon oncogenic H-Ras-induced senescence. As shown in Fig. 8B, SAP25 accumulated in the PML nuclear bodies upon Ras-induced senescence of human IMR-90 fibroblasts. Accumulation of SAP25 in the nucleus was also observed upon Ras-induced senescence of rat REF52 fibroblasts (data not shown). SAP25 may play a role in the regulation of cellular senescence through recruitment of mSin3-HDAC complex to the PML nuclear bodies.

Quantitative proteomic analysis of SAP25 complex. To gain more insight into the biochemical function of SAP25, we undertook a proteomic analysis of SAP25-containing protein

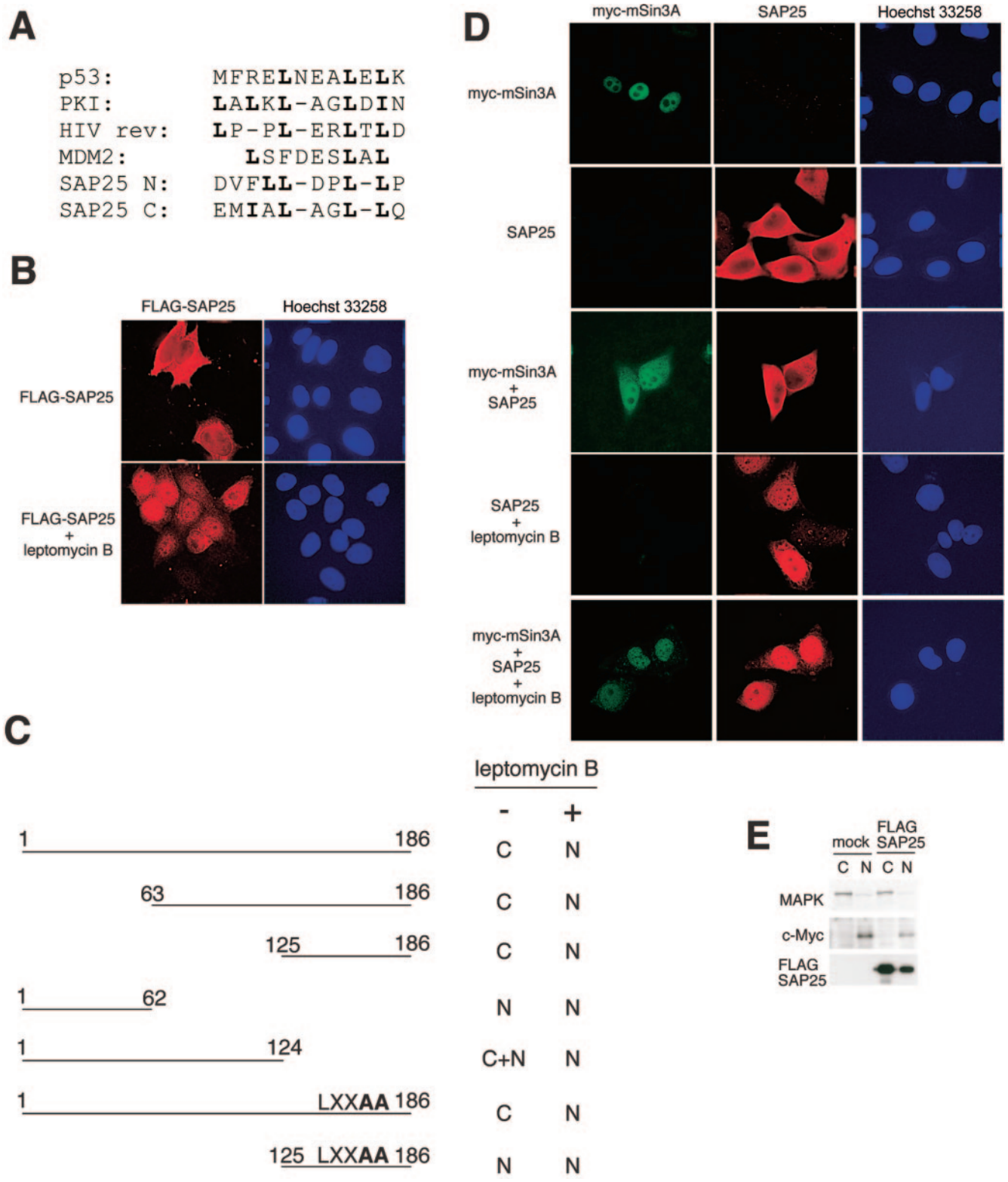

FIG. 7. Nuclear export of SAP25. (A) Alignment of the sequences of the LXXLL motifs in SAP25 and known leucine-rich nuclear export signals. (B) Subcellular location of FLAG-SAP25 in the presence or absence of leptomycin B. HeLa cells were transfected with FLAG-SAP25, and 24 h later the cells were either left untreated or treated with 5 ng/ml of leptomycin B for 24 h. The location of FLAG-SAP25 was determined by anti-FLAG indirect immunofluorescence. Nuclei were stained with Hoechst 33258. (C) Mapping of the nuclear export signals of SAP25. The subcellular location of the indicated deletion or substitution mutants of SAP25 was determined as in panel B. Predominant locations in the cytoplasm (C), the nucleus (N), or both (C+N) are indicated. More than 200 cells were examined for each location analysis. (D) Cytoplasmic sequestration of mSin3A by SAP25. HeLa cells were transfected with myc-tagged mSin3A, SAP25, or both, and their subcellular location was

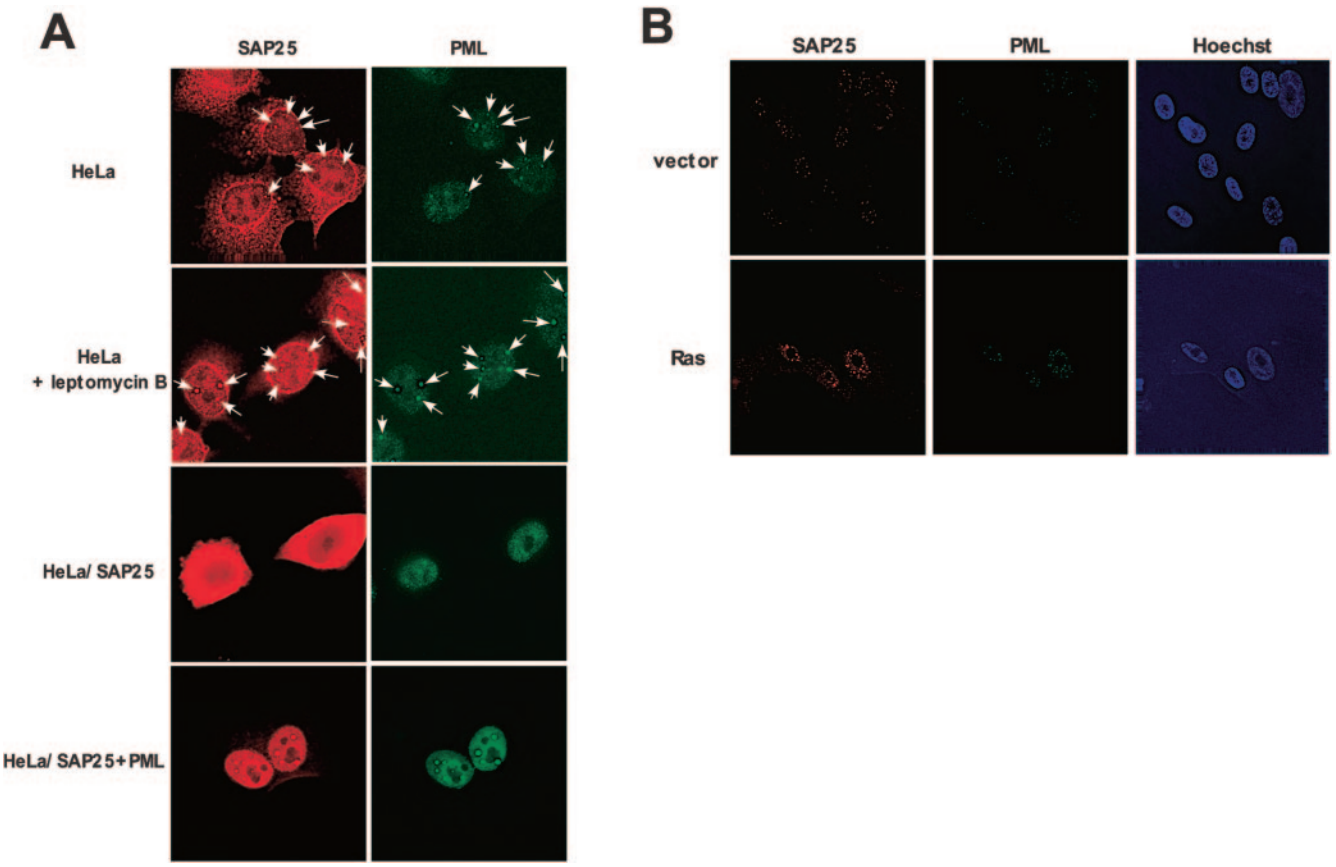

FIG. 8. Localization of SAP25 in PML nuclear bodies. (A) Localization of SAP25 in PML nuclear bodies in HeLa cells. Untreated HeLa cells or HeLa cells treated with 5 ng/ml of leptomycin B for 24 h were stained for SAP25 or PML (top and second rows). In untreated HeLa cells, SAP25 is mainly cytoplasmic, but a fraction of SAP25 is located in the nucleus and is concentrated in the nuclear dot-like structures that coincide with PML nuclear bodies (indicated by arrows, top row). Upon leptomycin B treatment, SAP25 accumulated in the nucleus and in PML nuclear bodies (indicated by arrows, second row). HeLa cells were transfected with SAP25 or SAP25 and PML. After 48 h, the cells were stained for SAP25 and PML (third and fourth rows). Transfected SAP25 was predominantly cytoplasmic (third row), but coexpression of PML caused accumulation of SAP25 in PML nuclear bodies and the nucleoplasm (fourth row). (B) Accumulation of SAP25 in PML nuclear bodies upon Ras-induced senescence of human IMR-90 fibroblasts. IMR-90 fibroblasts were infected with retroviruses expressing activated Ras or empty vector retroviruses. Infected cells were selected with puromycin for 2 days. Eight days after infection, the cells were stained for SAP25 and PML.

complexes. Since PML induces nuclear retention of SAP25 (Fig. 8A), we compared the components of the SAP25 complex in the presence or absence of PML coexpression by using ICAT (isotope-coded affinity tags) quantitative proteomics technology (16, 49) (Fig. 9). HeLa cells were transfected with FLAG-SAP25 alone or with FLAG-SAP25 and PML, and the cell lysates were immunoprecipitated with anti-FLAG antibody under nondenaturing conditions. The FLAG-SAP25 and its associated proteins were eluted with FLAG peptide and were labeled with the ICAT reagents (isotopically light ICAT for the FLAG-SAP25 sample and isotopically heavy ICAT for FLAG-SAP25-plus-PML sample). The two labeled samples were combined, proteolyzed to peptides with trypsin, and fractionated by cation-exchange chromatography. ICAT-labeled peptides were isolated by avidin affinity chromatography and were analyzed by microcapillary reversed-phase liquid chromatography–tandem mass spectrometry. The amino acid sequences of the peptides were determined by correlating the collision-induced dissociation spectra with a protein sequence database using the SEQUEST search algorithm (13). The relative abundance (FLAG-SAP25 alone versus FLAG-SAP25 plus PML) of an identified ICAT-labeled peptide pair was determined from the ratio of the peptide peaks using the ASAPRatio software tool (39).

As shown in Table 1, several components of the mSin3 corepressor complex such as mSin3A, mSin3B, *O*-GlcNAc transferase (OGT), SAP130, SAP30, RbAP46, and BRMS1 were

examined by anti-myc (9E10) and anti-SAP25 immunofluorescence. Nuclei were stained with Hoechst 33258. Where indicated, the transfected cells were treated with 5 ng/ml of leptomycin B. (E) Biochemical fractionation of SAP25-transfected cells. HeLa cells transfected with FLAG-SAP25 were fractionated into cytoplasmic and nuclear fractions by the method of Dignam et al. (12), and FLAG-SAP25 was detected by anti-FLAG immunoblotting. Anti-MAPK and anti-c-Myc immunoblots serve as fractionation controls.

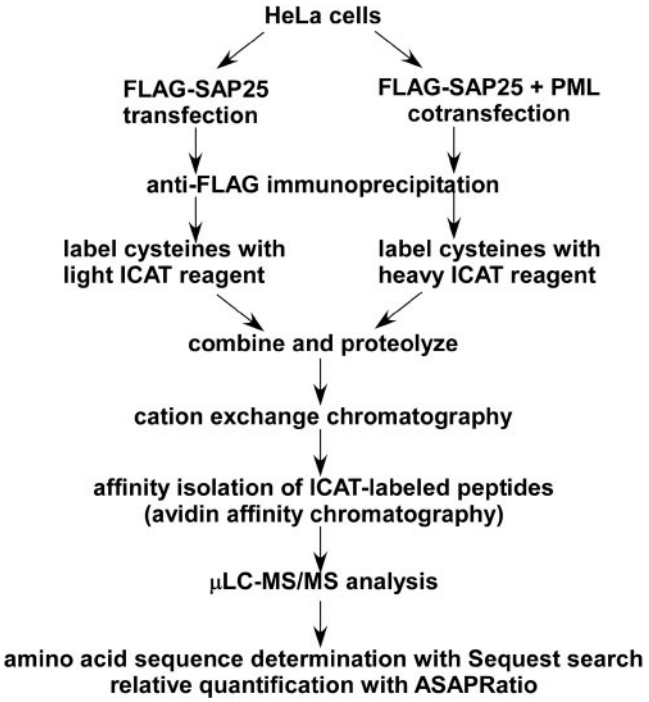

FIG. 9. ICAT proteomic analysis of the SAP25 complex. HeLa cells were transfected with FLAG-SAP25 or with FLAG-SAP25 and PML. The cell lysates were immunoprecipitated with anti-FLAG antibody under nondenaturing conditions. The two protein complexes were labeled with the ICAT reagents (light ICAT for the FLAG-SAP25 sample and heavy ICAT for the FLAG-SAP25-plus-PML sample). The two labeled protein complexes were combined, proteolyzed to peptides with trypsin, and fractionated by cation-exchange chromatography followed by avidin affinity chromatography. The purified ICAT-labeled peptides were analyzed by microcapillary liquid chromatography-tandem mass spectrometry (μLC-MS/MS) for amino acid sequence determination and relative quantification.

found associated with SAP25, which further supports the notion that SAP25 is a core component of the mSin3 complex. The expression of SAP25 was slightly enhanced in the presence of PML (without PML/with PML ratio, 0.85:1.00). PML enhanced the association of SAP25 and TFIIB, which may suggest a role of SAP25 in modulating the basal transcription machinery. Although dozens of proteins were shown to be located in PML nuclear bodies (11), PML nuclear bodies are not soluble under the nondenaturing conditions which preserve the protein complexes (41) and are likely not represented in our immunoprecipitation-ICAT proteomic analysis. This may explain the only modest effect of PML on the composition of SAP25 complex observed in our analysis (Table 1). The association of CRM1, seh1, and karyopherin β2, with SAP25 is likely to mediate the nucleocytoplasmic transport of SAP25. The association of CDK4 and its inhibitor, p16(INK4a), with SAP25 may suggest a role of SAP25 in the regulation of cell cycle.

DISCUSSION

mSin3A and mSin3B were first identified through their association with the Mad family of transcriptional repressors (4, 48), and subsequent work from many laboratories has shown them to be involved in multiple protein-protein interactions. Thus far, mSin3-associated proteins can be classified into the following three categories: The first class consists of enzymes that perform posttranslational modifications. These include HDAC1 and -2 (2, 18, 21, 23, 33, 42, 64), Swi/Snf chromatin remodeling complex subunits (52), O-linked *N*-acetylglucosamine transferase (62), and histone methyltransferases (43, 59). The second group comprises a large number of DNA-binding transcription factors that have been reported to bind mSin3. These include the Mad family repressors, MeCP2 (44), Ikaros (27), Pf1 (63), MNFβ (60), and Elk-1 (61). Third, a number of proteins associated with mSin3 appear to serve as docking proteins for specific repression components. For example, SDS3/SAP45 (1, 15, 37) mediates the association of HDAC1 and HDAC2 with Sin3 in both mammalian and yeast cells and SAP30 mediates the binding of mSin3 and N-CoR (32).

We have cloned and characterized the 25-kDa mSin3A-associated polypeptide, SAP25. SAP25 is a novel protein that binds to the PAH1 domain of mSin3A. SAP25 associates with mSin3-HDAC complex in vivo and is capable of repressing transcription when tethered to DNA. SAP25 does not display any significant homology to known enzymes. It does not have any recognizable DNA-binding motifs and does not display

TABLE 1. Proteins identified in the FLAG-SAP25 complex

Protein name	Protein probability score[a]	−PML:+PML[b]
TFIIB	1	0.11 ± 0.01:1.00
PML	1	0.15 ± 0.03:1.00
KIAA0153	0.93	0.37 ± 0.04:1.00
OGT	0.99	0.40 ± 0.03:1.00
mSin3A	1	0.49 ± 0.46:1.00
CDK4	1	0.78 ± 0.08:1.00
SAP25	1	0.85 ± 0.13:1.00
CRM1	0.98	0.88 ± 0.10:1.00
Zinc finger antiviral protein 1	1	0.89 ± 0.44:1.00
FLJ12443 protein	1	0.90 ± 0.32:1.00
Proliferation-inducing gene 21 protein	1	0.97 ± 0.18:1.00
DNJA2	1	1.00 ± 0.07:1.00
Replication factor C	1	1.00 ± 0.37:1.00
DNA-PKc	1	1.01 ± 0.12:1.00
Interferon-induced 56-kDa protein	1	1.04 ± 0.10:1.00
hnRNPI	1	1.04 ± 0.16:1.00
BRMS1	0.99	1.04 ± 0.20:1.00
Nucleoporin Seh1	1	1.16 ± 0.16:1.00
Karyopherin-2	0.99	1.23 ± 0.16:1.00
RbAP46	1	1.23 ± 0.20:1.00
hnRNPu	1	1.29 ± 0.58:1.00
SAP30	1	1.33 ± 0.06:1.00
p16(INK4a)	0.92	1.47 ± 0.89:1.00
Dead box protein 3	0.97	1.61 ± 0.31:1.00
hnRNPA1	0.98	1.86 ± 0.70:1.00
Interferon-induced 60-kDa protein	1	1.99 ± 0.11:1.00
Protein phosphatase 1Ac	1	2.27 ± 0.25:1.00
SAP130	1	Not quantifiable
mSin3B	0.99	Not quantifiable

[a] The proteins with a Protein Prophet probability score of 0.92 or higher are listed. In this experiment, a probability score of 0.92 corresponds to a false identification rate of 0.9% and 1.00 corresponds to a false identification rate of 0%.

[b] The relative abundance of each protein is compared for the FLAG-SAP25 (−PML) and FLAG-SAP25 plus PML (+PML) samples. For SAP130 and mSin3B, the identified peptides did not contain cysteines and were not quantifiable.

significant in vitro DNA-binding activities (Y. Shiio, unpublished data). Thus, it seems possible that SAP25 is a docking protein, perhaps permitting association between mSin3 and other repression components such as PML (see below).

The interaction of SAP25 with mSin3A is mediated by a C-terminal region of SAP25 including an LXXLL motif, and mutation of this motif abolished the interaction. The LXXLL motifs in other proteins have been implicated in the binding to nuclear hormone receptors and cyclin D1, but the LXXLL motif of SAP25 does not mediate interaction with these proteins and is specific to the PAH1 domain of mSin3. Another PAH1-binding domain in the POZ domain of PLZF also contains an LDDLL sequence (10). These LXXLL motifs may be a new class of LXXLL motifs that mediate the binding to mSin3 PAH1, but not to nuclear hormone receptors or cyclin D1. The PAH1-binding domain of SAP25 does not display any significant homology to other PAH1-binding domains of N-CoR (2, 21), Pf1 (63), and HCF (57). The mSin3-binding domain of SAP25 displays an order-of-magnitude-higher affinity to mSin3 PAH1 than the PAH1-binding domain of N-CoR (I. Radhakrishnan, personal communication) and may represent a unique PAH1 interaction domain. Nuclear magnetic resonance structural analysis of the complex between the mSin3A PAH1 domain and the SAP25 PAH1 interaction domain is currently under way (I. Radhakrishnan, unpublished data).

SAP25 is actively exported from the nucleus by a CRM1-dependent mechanism. SAP25 has at least two nuclear export signals, one of which overlaps with the PAH1-binding LXXLL motif (Fig. 7C). Quite divergent leucine-rich sequences were shown to function as CRM1-dependent nuclear export signals (29, 31). Compilation of 58 functional leucine-rich NES sequences indicated that only 36% of them fit the previously proposed NES consensus, L-x(2,3)-[LIVFM]-x(2,3)-L-x-[LI] (31). In fact, an optimal CRM1-binding sequence, identified by using a random peptide library, inhibited the release of the nuclear export complex from the nuclear pore complex, suggesting that leucine-rich nuclear export signals have evolved to be low affinity and divergent (29). The LXXLL motif of SAP25 may represent another example of a divergent, low-affinity CRM1-binding nuclear export signal, although the binding of SAP25 and CRM1 was nonetheless detectable by immunoprecipitation-ICAT analysis (Table 1). Several lines of evidence suggest a role of PML in the nucleocytoplasmic shuttling of SAP25. Endogenous SAP25 in HeLa cells is mainly cytoplasmic, but a fraction of SAP25 is located in PML nuclear bodies (Fig. 8A). Furthermore, treatment with leptomycin B, an inhibitor of CRM1-dependent nuclear export, induced accumulation of SAP25 in PML nuclear bodies (Fig. 8A). Coexpression of PML induced a striking accumulation of SAP25 in PML nuclear bodies and the nucleoplasm (Fig. 8A). PML expression is induced upon Ras-induced senescence of primary fibroblasts, and the PML nuclear bodies increase in size and number during this process (14, 46). Concomitant with enhanced PML expression, SAP25 accumulates in PML nuclear bodies upon Ras-induced senescence (Fig. 8B). Several proteins located in PML nuclear bodies such as p53 (34), MDM2 (34), TRADD (40), and RBCK1 (53) are nucleocytoplasmic shuttling proteins and accumulate in PML nuclear bodies upon leptomycin B treatment. The precise role of PML in the shuttling of these proteins is not clear, but PML itself also has a CRM1-dependent nuclear export signal (22) and is exported to the cytoplasm upon human immunodeficiency virus infection (54). SAP25 is a new member of the growing family of nucleocytoplasmic shuttling proteins that are located in PML nuclear bodies.

PML nuclear bodies are implicated in diverse cellular functions such as gene regulation, apoptosis, senescence, DNA repair, and antiviral response (11). There is also evidence that RNA polymerase II and its nascent transcripts localize in PML nuclear bodies, suggesting that active transcription takes place in these structures (35, 55). PML was shown to interact with multiple corepressors (mSin3A, N-CoR, and c-Ski) and HDAC1, and this interaction was proposed to mediate the transcriptional repression by Mad (26). SAP25 may recruit the mSin3-HDAC complex to PML nuclear bodies and modulate gene transcription. The enhanced association of TFIIB with SAP25 upon PML coexpression (Table 1) may also hint at a role of SAP25 in regulation of basal transcription. However, the role of SAP25 may not be limited to gene transcription. Recently, human Sir2 deacetylase was shown to be recruited to PML nuclear bodies and antagonize PML-induced acetylation of p53 and PML-induced cellular senescence (36). Similarly, SAP25 may recruit the mSin3-HDAC complex to PML nuclear bodies and induce deacetylation of p53 or some other key regulator(s), modulating cellular senescence. The association of SAP25 with CDK4 and p16(INK4a) (Table 1) may also suggest a nontranscriptional role for SAP25. In conclusion, we have identified a novel mSin3-binding protein, SAP25. SAP25 is a new class of core components of mSin3 complex, which is constantly shuttling between the nucleus and the cytoplasm and whose subcellular location is regulated by PML. The precise biochemical and biological role of SAP25 remains to be established, but the present findings suggest that it plays a regulatory role in repression of transcription.

ACKNOWLEDGMENTS

We thank Yoshiro Maru, Ed Seto, and Roel van Driel for antibodies and Shaun Cowley for estrogen receptor constructs. We are grateful to Ishwar Radhakrishnan for discussions and prepublication information.

This work was supported by NIH grant R37CA057138 (R.N.E.); by federal funding from the National Heart, Blood, and Lung Institute under contract N01-HV-28179 (R.A.); by the NCI-Japanese Foundation for Cancer Research Training Program in the U.S.-Japan Cooperative Cancer Committee (Y.S.); by the Interdisciplinary Research Training Fellowship from the Fred Hutchinson Cancer Research Center (Y.S.); and by a gift from Merck and Co. to the ISB. R.N.E. is a Research Professor of the American Cancer Society.

REFERENCES

1. **Alland, L., G. David, H. Shen-Li, J. Potes, R. Muhle, H.-C. Lee, H. Hou, Jr., K. Chen, and R. A. DePinho.** 2002. Identification of mammalian Sds3 as an integral component of the Sin3/histone deacetylase corepressor complex. Mol. Cell. Biol. **22:**2743–2750.
2. **Alland, L., R. Muhle, H. Hou, Jr., J. Potes, L. Chin, N. Schreiber-Agus, and R. A. DePinho.** 1997. Role for N-CoR and histone deacetylase in Sin3-mediated transcriptional repression. Nature **387:**49–55.
3. **Ayer, D. E., C. D. Laherty, Q. A. Lawrence, A. P. Armstrong, and R. N. Eisenman.** 1996. Mad proteins contain a dominant transcription repression domain. Mol. Cell. Biol. **16:**5772–5781.
4. **Ayer, D. E., Q. A. Lawrence, and R. N. Eisenman.** 1995. Mad-Max transcriptional repression is mediated by ternary complex formation with mammalian homologs of yeast repressor Sin3. Cell **80:**767–776.
5. **Blackwood, E. M., and R. N. Eisenman.** 1991. Max: a helix-loop-helix zipper protein that forms a sequence-specific DNA-binding complex with Myc. Science **251:**1211–1217.

6. **Brubaker, K., S. M. Cowley, K. Huang, L. Loo, G. S. Yochum, D. E. Ayer, R. N. Eisenman, and I. Radhakrishnan.** 2000. Solution structure of the interacting domains of the Mad-Sin3 complex: implications for recruitment of a chromatin-modifying complex. Cell **103:**655–665.
7. **Chomczynski, P., and N. Sacchi.** 1987. Single-step method of RNA isolation by acid guanidinium thiocyanate-phenol-chloroform extraction. Anal. Biochem. **162:**156–159.
8. **Cowley, S. M., B. M. Iritani, S. M. Mendrysa, T. Xu, P. F. Cheng, J. Yada, H. D. Liggitt, and R. M. Eisenman.** 2005. The mSin3A chromatin-modifying complex is essential for embryogenesis and T-cell development. Mol. Cell. Biol. **25:**6990–7004.
9. **Dannenberg, J.-H., G. David, S. Zhong, J. van der Torre, W. H. Wong, and R. A. DePinho.** 2005. mSin3A corepressor regulates diverse transcriptional networks governing normal and neoplastic growth and survival. Genes Dev. **19:**1581–1595.
10. **David, G., L. Alland, S. H. Hong, C. W. Wong, R. A. DePinho, and A. Dejean.** 1998. Histone deacetylase associated with mSin3A mediates repression by the acute promyelocytic leukemia-associated PLZF protein. Oncogene **16:** 2549–2556.
11. **Dellaire, G., and D. P. Bazett-Jones.** 2004. PML nuclear bodies: dynamic sensors of DNA damage and cellular stress. BioEssays **26:**963–967.
12. **Dignam, J. D., R. M. Lebovitz, and R. G. Roeder.** 1983. Accurate transcription initiation by RNA polymerase II in a soluble extract from isolated mammalian nuclei. Nucleic Acids Res. **11:**1475–1489.
13. **Eng, J., A. L. McCormack, and J. R. Yates.** 1994. An approach to correlate tandem mass spectral data of peptides with amino acid sequences in a protein database. J. Am. Soc. Mass Spectrom. **5:**976–989.
14. **Ferbeyre, G., E. de Stanchina, E. Querido, N. Baptiste, C. Prives, and S. W. Lowe.** 2000. PML is induced by oncogenic ras and promotes premature senescence. Genes Dev. **14:**2015–2027.
15. **Fleischer, T. C., U. J. Yun, and D. E. Ayer.** 2003. Identification and characterization of three new components of the mSin3A corepressor complex. Mol. Cell. Biol. **23:**3456–3467.
16. **Gygi, S. P., B. Rist, S. A. Gerber, F. Turecek, M. H. Gelb, and R. Aebersold.** 1999. Quantitative analysis of complex protein mixtures using isotope-coded affinity tags. Nat. Biotechnol. **17:**994–999.
17. **Han, D. K., J. Eng, H. Zhou, and R. Aebersold.** 2001. Quantitative profiling of differentiation-induced microsomal proteins using isotope-coded affinity tags and mass spectrometry. Nat. Biotechnol. **19:**946–951.
18. **Hassig, C. A., T. C. Fleischer, A. N. Billin, S. L. Schreiber, and D. E. Ayer.** 1997. Histone deacetylase activity is required for full transcriptional repression by mSin3A. Cell **89:**341–347.
19. **Heery, D. M., S. Hoare, S. Hussain, M. G. Parker, and H. Sheppard.** 2001. Core LXXLL motif sequences in CREB-binding protein, SRC1, and RIP140 define affinity and selectivity for steroid and retinoid receptors. J. Biol. Chem. **276:**6695–6702.
20. **Heery, D. M., E. Kalkhoven, S. Hoare, and M. G. Parker.** 1997. A signature motif in transcriptional co-activators mediates binding to nuclear receptors. Nature **387:**733–736.
21. **Heinzel, T., R. M. Lavinsky, T. M. Mullen, M. Soderstrom, C. D. Laherty, J. Torchia, W. M. Yang, G. Brard, S. D. Ngo, J. R. Davie, E. Seto, R. N. Eisenman, D. W. Rose, C. K. Glass, and M. G. Rosenfeld.** 1997. A complex containing N-CoR, mSin3 and histone deacetylase mediates transcriptional repression. Nature **387:**43–48.
22. **Henderson, B. R., and A. Eleftheriou.** 2000. A comparison of the activity, sequence specificity, and CRM1-dependence of different nuclear export signals. Exp. Cell Res. **256:**213–224.
23. **Kadosh, D., and K. Struhl.** 1997. Repression by Ume6 involves recruitment of a complex containing Sin3 corepressor and Rpd3 histone deacetylase to target promoters. Cell **89:**365–371.
24. **Kaelin, W. G., Jr., W. Krek, W. R. Sellers, J. A. DeCaprio, F. Ajchenbaum, C. S. Fuchs, T. Chittenden, Y. Li, P. J. Farnham, M. A. Blanar, D. M. Livingston, and E. K. Flemington.** 1992. Expression cloning of a cDNA encoding a retinoblastoma-binding protein with E2F-like properties. Cell **70:**351–364.
25. **Keller, A., A. I. Nesvizhskii, E. Kolker, and R. Aebersold.** 2002. Empirical statistical model to estimate the accuracy of peptide identifications made by MS/MS and database search. Anal. Chem. **74:**5383–5392.
26. **Khan, M. M., T. Nomura, H. Kim, S. C. Kaul, R. Wadhwa, T. Shinagawa, E. Ichikawa-Iwata, S. Zhong, P. P. Pandolfi, and S. Ishii.** 2001. Role of PML and PML-RARalpha in Mad-mediated transcriptional repression. Mol. Cell **7:**1233–1243.
27. **Koipally, J., A. Renold, J. Kim, and K. Georgopoulos.** 1999. Repression by Ikaros and Aiolos is mediated through histone deacetylase complexes. EMBO J. **18:**3090–3100.
28. **Kozak, M.** 1984. Compilation and analysis of sequences upstream from the translational start site in eukaryotic mRNAs. Nucleic Acids Res. **12:**857–872.
29. **Kutay, U., and S. Guttinger.** 2005. Leucine-rich nuclear-export signals: born to be weak. Trends Cell Biol. **15:**121–124.
30. **Kuzmichev, A., Y. Zhang, H. Erdjument-Bromage, P. Tempst, and D. Reinberg.** 2002. Role of the Sin3-histone deacetylase complex in growth regulation by the candidate tumor suppressor $p33^{ING1}$. Mol. Cell. Biol. **22:**835–848.
31. **la Cour, T., R. Gupta, K. Rapacki, K. Skriver, F. M. Poulsen, and S. Brunak.** 2003. NESbase version 1.0: a database of nuclear export signals. Nucleic Acids Res. **31:**393–396.
32. **Laherty, C. D., A. N. Billin, R. M. Lavinsky, G. S. Yochum, A. C. Bush, J. M. Sun, T. M. Mullen, J. R. Davie, D. W. Rose, C. K. Glass, M. G. Rosenfeld, D. E. Ayer, and R. N. Eisenman.** 1998. SAP30, a component of the mSin3 corepressor complex involved in N-CoR-mediated repression by specific transcription factors. Mol. Cell **2:**33–42.
33. **Laherty, C. D., W. M. Yang, J. M. Sun, J. R. Davie, E. Seto, and R. N. Eisenman.** 1997. Histone deacetylases associated with the mSin3 corepressor mediate mad transcriptional repression. Cell **89:**349–356.
34. **Lain, S., C. Midgley, A. Sparks, E. B. Lane, and D. P. Lane.** 1999. An inhibitor of nuclear export activates the p53 response and induces the localization of HDM2 and p53 to U1A-positive nuclear bodies associated with the PODs. Exp. Cell Res. **248:**457–472.
35. **LaMorte, V. J., J. A. Dyck, R. L. Ochs, and R. M. Evans.** 1998. Localization of nascent RNA and CREB binding protein with the PML-containing nuclear body. Proc. Natl. Acad. Sci. USA **95:**4991–4996.
36. **Langley, E., M. Pearson, M. Faretta, U. M. Bauer, R. A. Frye, S. Minucci, P. G. Pelicci, and T. Kouzarides.** 2002. Human SIR2 deacetylates p53 and antagonizes PML/p53-induced cellular senescence. EMBO J. **21:**2383–2396.
37. **Lechner, T., M. J. Carrozza, Y. Yu, P. A. Grant, A. Eberharter, D. Vannier, G. Brosch, D. J. Stillman, D. Shore, and J. L. Workman.** 2000. Sds3 (suppressor of defective silencing 3) is an integral component of the yeast Sin3 · Rpd3 histone deacetylase complex and is required for histone deacetylase activity. J. Biol. Chem. **275:**40961–40966.
38. **Li, J., Q. Lin, W. Wang, P. Wade, and J. Wong.** 2002. Specific targeting and constitutive association of histone deacetylase complexes during transcriptional repression. Genes Dev. **16:**687–692.
39. **Li, X. J., H. Zhang, J. A. Ranish, and R. Aebersold.** 2003. Automated statistical analysis of protein abundance ratios from data generated by stable-isotope dilution and tandem mass spectrometry. Anal. Chem. **75:**6648–6657.
40. **Morgan, M., J. Thorburn, P. P. Pandolfi, and A. Thorburn.** 2002. Nuclear and cytoplasmic shuttling of TRADD induces apoptosis via different mechanisms. J. Cell Biol. **157:**975–984.
41. **Muller, S., M. J. Matunis, and A. Dejean.** 1998. Conjugation with the ubiquitin-related modifier SUMO-1 regulates the partitioning of PML within the nucleus. EMBO J. **17:**61–70.
42. **Nagy, L., H. Y. Kao, D. Chakravarti, R. J. Lin, C. A. Hassig, D. E. Ayer, S. L. Schreiber, and R. M. Evans.** 1997. Nuclear receptor repression mediated by a complex containing SMRT, mSin3A, and histone deacetylase. Cell **89:**373–380.
43. **Nakamura, T., T. Mori, S. Tada, W. Krajewski, T. Rozovskaia, R. Wassell, G. Dubois, A. Mazo, C. M. Croce, and E. Canaani.** 2002. ALL-1 is a histone methyltransferase that assembles a supercomplex of proteins involved in transcriptional regulation. Mol. Cell **10:**1119–1128.
44. **Nan, X., H. H. Ng, C. A. Johnson, C. D. Laherty, B. M. Turner, R. N. Eisenman, and A. Bird.** 1998. Transcriptional repression by the methyl-CpG-binding protein MeCP2 involves a histone deacetylase complex. Nature **393:**386–389.
45. **Nesvizhskii, A. I., A. Keller, E. Kolker, and R. Aebersold.** 2003. A statistical model for identifying proteins by tandem mass spectrometry. Anal. Chem. **75:**4646–4658.
46. **Pearson, M., R. Carbone, C. Sebastiani, M. Cioce, M. Fagioli, S. Saito, Y. Higashimoto, E. Appella, S. Minucci, P. P. Pandolfi, and P. G. Pelicci.** 2000. PML regulates p53 acetylation and premature senescence induced by oncogenic Ras. Nature **406:**207–210.
47. **Pickering, B. M., and A. E. Willis.** 2005. The implications of structured 5′ untranslated regions on translation and disease. Semin. Cell Dev. Biol. **16:**39–47.
48. **Schreiber-Agus, N., L. Chin, K. Chen, R. Torres, G. Rao, P. Guida, A. I. Skoultchi, and R. A. DePinho.** 1995. An amino-terminal domain of Mxi1 mediates anti-Myc oncogenic activity and interacts with a homolog of the yeast transcriptional repressor SIN3. Cell **80:**777–786.
49. **Shiio, Y., S. Donohoe, E. C. Yi, D. R. Goodlett, R. Aebersold, and R. N. Eisenman.** 2002. Quantitative proteomic analysis of Myc oncoprotein function. EMBO J. **21:**5088–5096.
50. **Shiio, Y., and R. N. Eisenman.** 2003. Histone sumoylation is associated with transcriptional repression. Proc. Natl. Acad. Sci. USA **100:**13225–13230.
51. **Shiio, Y., R. N. Eisenman, E. C. Yi, S. Donohoe, D. R. Goodlett, and R. Aebersold.** 2003. Quantitative proteomic analysis of chromatin-associated factors. J. Am. Soc. Mass Spectrom. **14:**696–703.
52. **Sif, S., A. J. Saurin, A. N. Imbalzano, and R. E. Kingston.** 2001. Purification and characterization of mSin3A-containing Brg1 and hBrm chromatin remodeling complexes. Genes Dev. **15:**603–618.
53. **Tatematsu, K., N. Yoshimoto, T. Koyanagi, C. Tokunaga, T. Tachibana, Y. Yoneda, M. Yoshida, T. Okajima, K. Tanizawa, and S. Kuroda.** 2005. Nuclear-cytoplasmic shuttling of a RING-IBR protein RBCK1 and its functional interaction with nuclear body proteins. J. Biol. Chem. **280:**22937–22944. (First published 15 April 2005; doi:10.1074/jbc.M413476200.)
54. **Turelli, P., V. Doucas, E. Craig, B. Mangeat, N. Klages, R. Evans, G. Kalpana, and D. Trono.** 2001. Cytoplasmic recruitment of INI1 and PML on

incoming HIV preintegration complexes: interference with early steps of viral replication. Mol. Cell **7:**1245–1254.

55. **von Mikecz, A., S. Zhang, M. Montminy, E. M. Tan, and P. Hemmerich.** 2000. CREB-binding protein (CBP)/p300 and RNA polymerase II colocalize in transcriptionally active domains in the nucleus. J. Cell Biol. **150:**265–273.
56. **Wang, H., I. Clark, P. R. Nicholson, I. Herskowitz, and D. J. Stillman.** 1990. The *Saccharomyces cerevisiae SIN3* gene, a negative regulator of *HO*, contains four paired amphipathic helix motifs. Mol. Cell. Biol. **10:**5927–5936.
57. **Wysocka, J., M. P. Myers, C. D. Laherty, R. N. Eisenman, and W. Herr.** 2003. Human Sin3 deacetylase and trithorax-related Set1/Ash2 histone H3-K4 methyltransferase are tethered together selectively by the cell-proliferation factor HCF-1. Genes Dev. **17:**896–911.
58. **Xue, Y., J. Wong, G. T. Moreno, M. K. Young, J. Cote, and W. Wang.** 1998. NURD, a novel complex with both ATP-dependent chromatin-remodeling and histone deacetylase activities. Mol. Cell **2:**851–861.
59. **Yang, L., Q. Mei, A. Zielinska-Kwiatkowska, Y. Matsui, M. L. Blackburn, D. Benedetti, A. A. Krumm, G. J. Taborsky, Jr., and H. A. Chansky.** 2003. An ERG (ets-related gene)-associated histone methyltransferase interacts with histone deacetylases 1/2 and transcription co-repressors mSin3A/B. Biochem. J. **369:**651–657.
60. **Yang, Q., Y. Kong, B. Rothermel, D. J. Garry, R. Bassel-Duby, and R. S. Williams.** 2000. The winged-helix/forkhead protein myocyte nuclear factor beta (MNF-beta) forms a co-repressor complex with mammalian sin3B. Biochem. J. **345:**335–343.
61. **Yang, S.-H., E. Vickers, A. Brehm, T. Kouzarides, and A. D. Sharrocks.** 2001. Temporal recruitment of the mSin3A-histone deacetylase corepressor complex to the ETS domain transcription factor Elk-1. Mol. Cell. Biol. **21:**2802–2814.
62. **Yang, X., F. Zhang, and J. E. Kudlow.** 2002. Recruitment of O-GlcNAc transferase to promoters by corepressor mSin3A: coupling protein O-GlcNAcylation to transcriptional repression. Cell **110:**69–80.
63. **Yochum, G. S., and D. E. Ayer.** 2001. Pf1, a novel PHD zinc finger protein that links the TLE corepressor to the mSin3A-histone deacetylase complex. Mol. Cell. Biol. **21:**4110–4118.
64. **Zhang, Y., R. Iratni, H. Erdjument-Bromage, P. Tempst, and D. Reinberg.** 1997. Histone deacetylases and SAP18, a novel polypeptide, are components of a human Sin3 complex. Cell **89:**357–364.
65. **Zhang, Y., Z. W. Sun, R. Iratni, H. Erdjument-Bromage, P. Tempst, M. Hampsey, and D. Reinberg.** 1998. SAP30, a novel protein conserved between human and yeast, is a component of a histone deacetylase complex. Mol. Cell **1:**1021–1031.
66. **Zwijsen, R. M., R. S. Buckle, E. M. Hijmans, C. J. Loomans, and R. Bernards.** 1998. Ligand-independent recruitment of steroid receptor coactivators to estrogen receptor by cyclin D1. Genes Dev. **12:**3488–3498.